IEEE Access
Multidisciplinary | Rapid Review | Open Access Journal

Received 29 March 2024, accepted 12 April 2024, date of publication 16 April 2024, date of current version 23 April 2024.

Digital Object Identifier 10.1109/ACCESS.2024.3389823

RESEARCH ARTICLE

Optimizing PAPR, BER, and PSD Efficiency: Using Phase Factors Generated by Bacteria Foraging Algorithm for PTS and SLM Methods

ARUN KUMAR[1], (Member, IEEE), NISHANT GAUR[2], AND AZIZ NANTHAAMORNPHONG[3], (Member, IEEE)

[1]Department of Electronics and Communication Engineering, New Horizon College of Engineering, Bengaluru 560103, India
[2]Department of Physics, JECRC University, Jaipur 303905, India
[3]College of Computing, Prince of Songkla University, Phuket 83120, Thailand

Corresponding author: Aziz Nanthaamornphong (aziz.n@phuket.psu.ac.th)

ABSTRACT The orthogonal time–frequency space (OTFS) waveform is a modulation scheme for wireless communication that achieves high spectral efficiency by exploiting multipath propagation, offering robustness to Doppler shifts and delay spread. A high peak-to-average power ratio (PAPR) is considered to be a significant issue in the OTFS waveform, drastically reducing the performance of the framework. PAPR affects system performance by causing power amplifiers to operate inefficiently at high power levels, leading to increased power consumption, distortion, and reduced spectral efficiency. In this study, we combined the partial transmission sequence (PTS) and selective mapping (SLM) with the bacterial foraging algorithm (BFA), which is also known as the SLM-BFA and PTS-BFA. An extensive search for the optimal phase factors in the PTS and SLM can be computationally expensive. BFO mimics the foraging behavior of bacteria to efficiently navigate the search space. BFO intelligently finds the optimal phase factors, reducing the computation and PAPR values of the OTFS. The performance of the proposed hybrid schemes was simulated for Rayleigh and Rician channels for 64 and 256 subcarriers, respectively. Parameters such as PAPR, bit error rate (BER), and power spectral density (PSD) were analyzed and compared with those of conventional SLM and PTS methods. The projected hybrid methods obtained a significant PAPR gain of 7.9 and 11.9 dB for 64 subcarriers and 7.5 dB and 8.9 dB for 256 subcarriers with Rayleigh and Rician channels, respectively. Further, it is seen that the proposed methods effectively retained the BER performance of the framework with trivial intricacy. In conclusion, using PTS and SLM techniques, which have been improved by the BFA, makes OTFS waveform communication systems work better. These methods effectively mitigate the PAPR issue and improve the system efficiency and spectral utilization. The synergy between the PTS, SLM, and BFA offers a promising approach for overcoming the challenges in OTFS modulation, contributing to the advancement of robust and efficient wireless communication technologies.

INDEX TERMS PAPR, OTFS, PTS-BFA, SLM-BFA, BER, PSD.

I. INTRODUCTION

The Orthogonal Time Frequency Space (OTFS) waveform emerged as an innovative modulation approach, capturing the interest of researchers owing to its distinctive qualities and prospective benefits in the realm of wireless communications. For thorough appreciation, it is instructive to explore the underpinnings, technical intricacies, and merits of the OTFS waveform [1]. In contrast to traditional wireless systems, such as orthogonal frequency division multiplexing (OFDM), OTFS excels in highly dynamic settings or those characterized by intense multipath effects. The conventional hindrances of OFDM, notably inter-symbol interference (ISI) and inter-carrier interference (ICI), tend to impair system efficacy, particularly at high velocities where these issues are most pronounced. The proposed OTFS waveform

The associate editor coordinating the review of this manuscript and approving it for publication was Xijun Wang.

solves these challenges by decoupling time and frequency dimensions. This means that the waveform is not bound to a fixed time-frequency grid, as in OFDM, but rather spreads information over a 2D grid in time and delay-Doppler space [2]. OTFS modulation decouples the symbols onto a 2D delay-Doppler grid, effectively separating the effects of time and frequency spreading. This grid provides resilience against the time-varying channel conditions encountered in high-mobility scenarios. Moreover, OTFS employs sophisticated processing algorithms such as the 2D Fourier transform to efficiently recover the transmitted symbols and mitigate the effects of ISI and ICI. The OTFS waveform is well-suited for high-mobility scenarios, such as vehicular communications and airborne platforms [3]. Its ability to decouple the time and frequency dimensions enables robust performance, even at high velocities, where traditional modulation schemes struggle. By spreading the information across both time- and delay-Doppler dimensions, OTFS can achieve a higher spectral efficiency than conventional modulation techniques such as OFDM. This increased efficiency is particularly beneficial in bandwidth-limited environments because it allows more data to be transmitted within the available spectrum [4]. The OTFS waveform exhibits improved coverage and penetration capabilities in challenging environments, including urban areas with tall buildings and indoor scenarios with multipath reflections. Its resilience to multipath propagation and time-varying channels enhances the reliability of communication links, even under non-line-of-sight conditions. Despite employing sophisticated signal processing strategies, the OTFS waveform provides the advantage of less complex equalization than other advanced modulation methods. This attribute renders it practical for deployment in systems requiring real-time processing, such as mobile and Internet of Things (IoT) devices, which often have a constrained computational capacity [5]. The OTFS can be integrated with existing wireless communication standards, offering a backward-compatible solution for upgrading legacy systems. This compatibility facilitates the adoption of OTFS in practical deployments without requiring a complete overhaul of infrastructure or devices. The OTFS waveform is a promising modulation technique that addresses the challenges posed by the high mobility environments and time-varying channels in wireless communication systems. Its unique properties, including resilience to multipath propagation, improved spectral efficiency, and low-complexity equalization,make it a key technology in next-generation wireless networks [6]. In OTFS modulation, the peak-to-average power ratio (PAPR) problem arises because of the nature of the time-frequency spreading of the waveform. The OTFS spreads information across both time and delay-Doppler dimensions, which can lead to significant variations in the amplitude of the signal over time. Consequently, the peak power of the transmitted signal can significantly exceed its average power, resulting in suboptimal power amplifier function and the possibility of signal distortion. The challenge of a high PAPR in OTFS lies in maintaining signal integrity while minimizing power consumption and ensuring compatibility with hardware constraints [7]. A high PAPR requires power amplifiers with sufficient headroom to accommodate peak power levels, reduce efficiency, and increase system cost. Various techniques can be employed to mitigate the PAPR problem in OTFS, including peak power reduction algorithms such as clipping and filtering, or the use of specific coding schemes optimized for reducing PAPR. Additionally, advanced digital predistortion techniques can be applied to compensate for the nonlinearities introduced by power amplifiers operating at high PAPR levels [8]. Managing the PAPR in OTFS is crucial for optimizing power efficiency and maintaining signal quality in wireless communication systems. PAPR reduction algorithms employing genetic algorithms iteratively evolve signal parameters to minimize the PAPR in OTFS modulation. Genetic algorithm mimic-neural selection generates diverse solutions and iteratively selects and combines them to optimize the waveform characteristics [9]. By intelligently adjusting parameters, such as symbol allocation and phase adjustments, genetic algorithms effectively reduce PAPR while maintaining signal quality. This approach harnesses computational intelligence to tackle the PAPR challenge in OTFS, thereby enhancing the system performance and efficiency. The proposed work combines the Bacteria Foraging Algorithm (BFA) [10] with partial transmission sequence (PTS) and selective mapping (SLM) techniques to enhance PAPR performance in OTFS modulation. Inspired by bacterial foraging behavior, BFA optimizes the signal parameters by iteratively adjusting the phase factors to minimize the PAPR. When combined with PTS and SLM, BFA efficiently explores the solution space and finds optimal phase sequences and constellation mappings that further reduce the PAPR. This integrated approach exploits the benefits of biological-inspired optimization along with conventional PAPR reduction methods, thereby significantly improving the performance of OTFS systems.

In [11], a composite technique that integrates PTS and SLM was developed. This study focuses on evaluating the performance of NOMA in terms of PAPR, bit error rate (BER), and power spectral density (PSD) by employing the proposed amalgamated SLM+PTS technique supplemented by a complementary reduction strategy. A subsequent analysis of the complexity revealed that this integrated technique yields optimal BER and PAPR results with minimal complexity. Notably, the hybrid techniques managed to curtail the PAPR to 3.1 dB while also achieving a gain of 4.34 dB and a power efficiency improvement of 34%. The research outlined in [12] validates the efficiency of the proposed SLM-PTS-CT technique for PAPR reduction within the O-NOMA waveforms. By integrating SLM, PTS, and CT techniques, a considerable decrease in PAPR is achieved, leading to enhanced power efficiency and overall system performance. Furthermore, BER analysis

revealed a significant reduction in errors, which signifies an improvement in signal quality and reliability. Moreover, the analysis of the PSD indicated a smoother and more uniform spectrum, reducing the risk of interference with adjacent channels and mitigating spectrum regrowth issues. In [13], a PAPR subtraction technique involving the use of precoding and Dummy Sequence Insertion (DSI) was introduced as a solution to these challenges. In addition, a specialized procedure for generating dummy sequences was developed, specifically tailored for the proposed method. We show that the method we developed achieves superior outcomes in terms of BER performance and PAPR reduction compared to methods based on precoding and PTS. Additionally, it requires significantly less computational effort than PTS techniques. The authors of [14] proposed a unique SLM technique for OFDM-NOMA systems for PAPR reduction. The proposed SLM scheme uses the OFDM-NOMA transmitter structure to perform similarly to the conventional SLM scheme with reduced computing complexity. Numerous studies have been conducted on combining NOMA and OFDM systems, or OFDM-NOMA systems, to exploit the technological maturity of OFDM systems and enhance system performance. However, this also provides the system with high PAPR. This must be addressed, because a high PAPR lowers the power efficiency of the system. The study in [15] examined the decrease in PAPR using a hybrid approach that combined clipping and filtering with precoding using the Hartley Transform. The authors in [16] applied an adaptive particle swarm optimization technique within a PTS framework to mitigate the issue of high PAPR. The proposed method efficiently identifies the optimal set of phase-rotation factors, thereby reducing computational complexity. The experimental results indicate that this strategy significantly reduces both the computational burden and PAPR. This study provides a detailed analysis of various PAPR reduction techniques applied to DJSCC systems. In the research presented in [17], a variety of PAPR reduction strategies were explored, including cutting-edge deep learning-based approaches such as PAPR loss minimization and retraining post-clipping, along with more established techniques such as clipping, companding, SLM, and PTS. Our comparative study indicates that although traditional PAPR reduction methods are applicable to systems with separate source and channel coding, their performance within the DJSCC framework deviates from that of conventional systems. The study in [18] introduces an innovative NN-based technique aimed at reducing the PAPR in OFDM systems. This technique incorporates a PAPR reduction module that leverages neural networks to conform to the SLM procedure, ultimately minimizing the PAPR of the signal. The simulation results demonstrate the efficacy of the scheme based on 100 MHz OFDM signal. This plan can achieve a linearization effect following DPD processing of the low-PAPR signal. For 0.01 CCDF, this technique can provide a 4.5 dB PAPR reduction. The PAPR is the main drawback of the OFDM scheme in [19]. As the OFDM signal passed through the amplifier, the output of the device decreased because of the high PAPR. The PAPR in OFDM signals can be reduced by combining exponential and μ-law companding. Implementing the CCDF function in the companding approach lowers PAPR in OFDM systems. Compared with a previously published work, the application of the suggested BFO algorithm in [20] showed a significant decrease in the PAPR value with an increase in the accuracy of the OFDM system. It was discovered that the level of complexity was lower when compared and validated against the standard PTS technology. Thus, BFO is more computationally efficient than the standard PTS. While effective, the PTS approach is known for its high computational complexity stemming from an exhaustive search for the best phase factors. To address this limitation, the method was augmented by using a scaled-down version of the particle swarm optimization algorithm. This enhancement facilitates a more rapid and computationally efficient discovery of optimal phase factors that contribute to lower PAPR [21]. In the traditional particle swarm optimization (PSO) algorithm, the introduction of a scaling factor into the velocity update equation enhances the inertia, weight, and velocity of the particle, leading to accelerated convergence towards the optimal solution and an efficient reduction in the PAPR. The simulation results indicate that the proposed scaled PSO-PTS algorithm effectively diminishes PAPR and is particularly advantageous for applications utilizing 64-QAM modulation. In [22], the authors implemented PSO and GA to reduce the output power envelope fluctuation of the OFDM system to ameliorate the PAPR. A brief description of the PAPR and PTS methods in OFDM systems is provided. With the aid of a traditional PTS based on PSO and GA, we present an OFDM system. According to the simulation result, both evolutionary techniques perform better at lowering the PAPR than the traditional PTS OFDM. The contributions of this study are as follows:

- To the best of our knowledge, this is the first instance in which the SLM-BFA and PTS-BFA algorithms have been employed to mitigate PAPR in an OTFS waveform.
- By leveraging the optimization power of BFO, the synergistic combination of SLM and PTS achieves substantial PAPR improvement, leading to efficient BER and PSD performance compared to conventional algorithms with low computational complexity.
- It should also be noted that the proposed hybrid algorithms can be adapted to work with various symbol constellations used in the OTFS, ensuring broader applicability.
- The proposed PTS-BFO and SLM-BFO exhibited a significant PAPR reduction in the OTFS. Their strengths and potential for synergistic combination make them suitable tools for researchers and engineers to explore PAPR performance in OTFS-based communication systems.

The structure of the article is as follows: Section I introduces the topic by discussing the challenges associated with peak power in transmission and reviews PAPR reduction

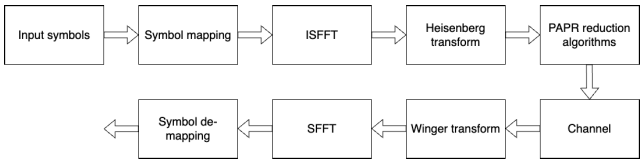

FIGURE 1. Block of OTFS waveform.

techniques. In Section II, we describe the system models for both the proposed and the existing algorithms. Section III presents a detailed analysis of the effects on the PAPR, BER, and PSD within the Rayleigh and Rician channels, specifically for the 64 and 256 subcarrier configurations. This article concludes in Section IV.

II. SYSTEM MODEL

The OTFS waveform block diagram comprises the receiver processing, two-dimensional (2D) modulation, pulse shaping, and symbol mapping. First, the symbols are mapped in the time-delay Doppler domain onto a 2D grid. The transmitted waveform is subsequently shaped by applying pulse-shaping filters to the symbols. Information is dispersed throughout the time and frequency dimensions of the modulated signal through 2D modulation. 2D demodulation was used for processing at the receiver to recover the transmitted symbols. The basic steps of the OTFS waveform transmission and reception are depicted in this block diagram, allowing for reliable communication in high-mobility settings under variable channel conditions [23]. A schematic of OTFS is shown in Fig. 1.

Let $X(\tau, f)$ be the transmitted OTFS signal in the time-delay Doppler domain. The instantaneous power of signal $P(\tau, f)$, at each point can be calculated as the square of its magnitude [24]:

$$P(\tau, f) = |X(\tau, f)|^2 \tag{1}$$

To determine PAPR, the ratio of the peak power to the average power of the signal must be computed. The peak power represents the highest instantaneous power measured over the entire time-frequency domain. Conversely, the average power, denoted as P_{avg}, is the average of the power levels across all points in that domain.

$$P_{\text{peak}} = \max_{\tau,f} P(\tau, f) \tag{2}$$

$$P_{\text{avg}} = \frac{1}{T \cdot F} \int_0^T \int_{-\infty}^{\infty} P(\tau, f)\, d\tau\, df \tag{3}$$

where T is the total duration in the delay domain, and F is the total bandwidth in the Doppler domain. Finally, the PAPR is given by

$$\text{PAPR} = \frac{P_{\text{peak}}}{P_{\text{avg}}} = \frac{\max_{\tau,f} P(\tau, f)}{\frac{1}{T \cdot F} \int_0^T \int_{-\infty}^{\infty} P(\tau, f)\, d\tau\, df} \tag{4}$$

The PAPR in dB is expressed as:

$$\text{PAPR}_{\text{dB}} = 10 \log_{10} \left(\frac{\max_{\tau,f} P(\tau, f)}{\frac{1}{T \cdot F} \int_0^T \int_{-\infty}^{\infty} P(\tau, f)\, d\tau\, df} \right) \tag{5}$$

A. PTS ALGORITHM

The Partial Transmit Sequence (PTS) method is widely used to reduce the PAPR in OFDM systems. This approach involves segmenting the initial data stream into several sub-blocks and assigning distinct phase sequences to each subblock [25]. Spreading the peak power throughout the sub-blocks effectively diminished the total PAPR. The original data stream X is divided into L sub-blocks, each denoted by x_l, where $l = 1, 2, \ldots, L$:

$$X = [x_1, x_2, \ldots, x_L] \tag{6}$$

For each sub-block l, M different phase sequences are generated, denoted by φ_l^m, where $m = 1, 2, \ldots, M$:

$$\varphi_l^m = \left[\varphi_l^{m(1)}, \varphi_l^{m(2)}, \ldots, \varphi_l^{m(N)} \right] \tag{7}$$

Each phase sequence is applied to the corresponding sub-block using complex exponential modulation [26]:

$$s_l^{m(k)} = x_{l(k)} * \exp(j * \varphi_l^{m(k)}), \quad k = 1, 2, \ldots, N \tag{8}$$

$s_l^{m(k)}$ denotes the k-th subcarrier of the m-th candidate signal for sub-block l. The candidate signal that exhibited the minimum PAPR was selected for transmission for each sub-block.

$$l_{\text{opt}} = \arg\min_m PAPR(s_l^m) \tag{9}$$

where l_{opt} is the index of the chosen candidate for sub-block l, and $PAPR(s_l^m)$ is the PAPR of the m-th candidate signal. The chosen candidate signals from each sub-block are combined to form the final transmitted signal S [27]:

$$S(k) = \sum_{l=1}^{L} s_l^{(l_{\text{opt}})}(k) \tag{10}$$

B. SLM

SLM is employed to reduce the PAPR in OTFS modulation systems. SLM employs various phase sequences to generate numerous versions of the transmitted signal corresponding to the data symbols. After merging these versions, each version was assigned a weight and adjusted to reduce the PAPR of the combined signals. The SLM efficiently redistributes the maximum power of the transmitted signal by carefully choosing the phase sequences and weighting factors [28]. This reduces the chances of signal distortion and nonlinear effects in the transmitter and amplifier components. Within the framework of the OTFS, the SLM technique adjusts itself to the unique properties of the signal. SLM effectively reduces the PAPR without compromising the spectral efficiency using built-in redundancy in the modulation scheme. The adaptability of SLM makes it a promising solution for reducing the high PAPR problem

in OTFS systems, thereby improving their performance under real-world communication circumstances [29]. Let us represent the OTFS symbol x(t) as

$$x(t) = \sum_{n} c_n * p_n(t - nT) \tag{11}$$

c_n is the complex data symbol on subcarrier n, $p(t)$ is the time-domain pulse shape for subcarrier n, and T is the subcarrier spacing. The PAPR is given by

$$PAPR(x) = \frac{\max(|x(t)|^2)}{E(|x(t)|^2)} \tag{12}$$

Let K be the number of candidate signal versions (mapping sets), and we define a mapping matrix $\mathbf{M}_k$ for each version, where each row represents a mapping for one data symbol to subcarriers represented by

$$M_k = [m_{1k}, m_{2k}, \ldots, m_{Nk}] \tag{13}$$

m_n^k denotes the subcarrier index (among the available N) where the nth data symbol is mapped in the k-th version. Each mapping matrix $\mathbf{M}_k$ generates the corresponding candidate signal, as follows

$$x_k(t) = \sum_{n} c_n * p_{m_n^k}(t - m_n^k T) \tag{14}$$

The candidate with the minimum PAPR for transmission is given by

$$x_t = \arg\min_{k} PAPR(x_k(t)) \tag{15}$$

C. BACTERIA FORAGING ALGORITHM

The Bacteria Foraging Algorithm (BFA) draws inspiration from the foraging behavior exhibited by bacteria and serves as a computer optimization method. ''Virtual bacteri'' within the framework of BFA imitate the movement and interactions found in bacterial colonies during foraging to depict the problem's potential solutions. Every bacterium embodies a prospective resolution, and its location correlates with a potential solution within the problem domain [30]. Bacteria exhibit chemotactic, swarming, and reproductive behaviors and seek more favorable conditions. Chemotaxis is where bacteria navigate towards areas with higher concentrations of ''food,'' which corresponds to more optimal solutions in the optimization problem. Swarming promotes communal exploration of the search space by bacteria, whereas reproduction enables potential strategies to generate offspring with minor alterations. The application of BFA has proven successful in a wide range of optimization challenges, such as engineering design, image processing, and machine learning. The significance of this resides in its capacity to effectively investigate intricate solution spaces, adjust to changing circumstances, and discover top-notch answers in a wide variety of optimization jobs. The BBFA does not have a single monolithic mathematical model, but relies on multiple interconnected equations capturing different aspects of bacterial behavior [31]. The Bacterial Foraging Algorithm (BFA) is an optimization method that draws inspiration from the natural foraging strategies of bacterial species. The mathematical equations governing BFA are primarily derived from the behaviors exhibited by bacterial colonies as they search for food sources. Chemotaxis: Bacteria adjust their positions towards higher food concentrations (better solutions). The following equation determines the movement of each bacterium x_i [32]:

$$x_i(t+1) = x_i(t) + \Delta x_i \tag{16}$$

where Δx_i is the movement step size calculated based on the concentration gradient of the objective function, and bacteria exhibit swarming behavior to collectively explore the search space. The new position of a bacterium is influenced by the position of the nearby bacteria, which promotes exploration and exploitation. The swarm movement equation can be represented as

$$x_i(t+1) = x_i(t) + \sum_{j=1}^{N} \beta_{ij}(x_j(t) - x_i(t)) \tag{17}$$

where β_{ij} is the interaction coefficient between bacteria i and j, and N is the total number of bacteria. In the next step, promising bacteria reproduce to produce offspring with slight variations. The reproduction equation involves perturbing the positions of the selected bacteria to introduce diversity in the population, as given by

$$x_i(t+1) = x_i(t) + \delta_i \tag{18}$$

where δ_i represents a small perturbation vector, it is also noted that parameters like population size, movement step size, interaction coefficients, and perturbation factors govern the dynamics of the BFA and enable it to efficiently explore the solution space and find optimal or near-optimal solutions for various optimization problems [33]. BFA stands out among the various optimization algorithms owing to its unique biological inspiration and effective problem-solving capabilities. Unlike many other algorithms, BFA mimics the foraging behavior of bacterial colonies, enabling it to efficiently navigate complex search spaces. This biological analogy imbues the BFA with adaptability, robustness, and scalability, making it particularly adept at solving optimization problems across diverse domains. Moreover, BFA's decentralized nature of BFA allows parallel processing, thereby enhancing its computational efficiency. In addition, the BFA exhibits a balance between exploration and exploitation, ensuring thorough exploration of the search space while exploiting promising regions for optimal solutions. Its simplicity, ease of implementation, and ability to handle high-dimensional problems further contributes to its appeal. Overall, the biological grounding and versatile performance of BFA make it a promising choice for optimization tasks, outshining many other algorithms in terms of efficacy and applicability. Algorithm 1 shows the pseudo code for the BFA. Selecting the parameters for the BFA in the PTS and SLM methods requires careful tuning. We began by adjusting the chemotaxis step

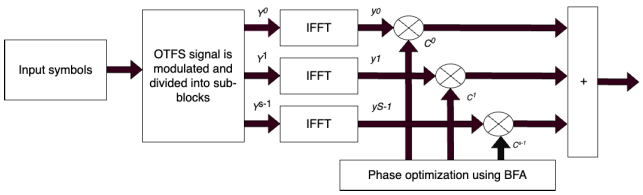

FIGURE 2. PTS-BFA.

size to balance exploration and exploitation. The elimination dispersal parameters were set to control bacterial dispersal and elimination rates, aiding in population diversity. Fine-tuning of reproductive steps to regulate bacterial reproduction rates. Finally, we optimize the swim length and tumble step to enhance the search efficiency. These parameters were iteratively adjusted based on the performance metrics for the optimal results.

D. PROPOSED PTS-BFA

The hybridization of PTS with BFA offers several benefits for reducing PAPR in OTFS modulation systems. PTS efficiently reduces the PAPR by decomposing the signal into disjoint subsets and optimizing the phase factors of each subset. However, more than PTS is required to guarantee global optimality or to handle large search spaces effectively. By incorporating BFA, the hybrid approach enhances the effectiveness of the PAPR reduction by exploring the solution space more comprehensively. BFA's ability of the BFA to adaptively search for optimal solutions while considering the interactions among signal segments helps in efficiently finding better solutions.

Additionally, BFA's ability of the BFA to handle dynamic environments and its inherent robustness further improve the reliability of PAPR reduction. Overall, the hybrid PTS with BFA combines the strengths of both techniques, providing a more effective and robust solution for mitigating PAPR in OTFS modulation systems. The drawbacks of the hybrid PTS with BFA include increased computational complexity owing to the combination of the two optimization techniques. In addition, tuning the parameters of both the PTS and BFA for optimal performance can be challenging and requires careful consideration and intensive computational resources. A schematic of the PTS-BFA is shown in Fig. 2. The proposed algorithm consists of several critical steps. Initially, the OTFS signal is divided into a series of blocks. These blocks are then processed with phase weighting and subjected to IFFT operations. Subsequently, a selection mechanism is applied to identify the block that exhibits the lowest Peak to PAPR. The final step involves amalgamating the chosen blocks to construct the final output signal. This iterative methodology effectively minimizes the PAPR, thereby boosting the operational efficiency and reliability of OFDM communication systems.

Algorithm 1 Pseudo Code of BFA

Initialization:
Define the problem with its objective function (fitness measure).
Population size: 100-200.
Interaction coefficients: 0.1-0.5.
Movement step size: Often starts large and decreases over iterations.
Perturbation factors: 0.01-0.05.
Initialize each bacterium with a random position and health value (based on initial fitness).
Chemotaxis loop:
for each bacterium **do**
    Calculate attractant and repellent values based on nearby solutions and objective functions.
    Decide between attractant and repellent movement based on probabilities.
    Perform a "tumble" (random step) if attracted or repelled.
    Evaluate fitness of new position.
    Update attractant and repellent values based on new fitness.
end for
Perform this loop for a predetermined number of chemotaxis steps.
Swarming:
Implement cell-to-cell communication rules (e.g., healthy bacteria share information with neighbors).
Update bacterial positions based on shared information (optional).
Reproduction:
Select healthy bacteria for reproduction based on their fitness.
Create copies of selected bacteria (with potential mutations in their positions).
Update health values of newly created bacteria based on initial fitness evaluation.
Elimination-dispersal:
Calculate the elimination probability for each bacterium based on its health.
Eliminate some bacteria based on their probabilities.
Disperse some healthy bacteria to random positions in the search space.
Main loop:
Repeat Chemotaxis, Swarming, Reproduction, and Elimination-dispersal loops for a certain number of iterations.
Keep track of the best solution (highest fitness) in each iteration.
Termination:
Stop after reaching a predefined stopping criterion (e.g., maximum iterations, convergence).
Return the best solution found.

Let us consider an OTFS symbol x(t) with N subcarriers:

$$x(t) = \sum_{n} c_n * p_n(t - nT) \tag{19}$$

PTS creates M copies with different phase rotations:

$$x_m(t) = \sum_{n} \exp(j\phi_m(n)) * c_n * p_n(t - nT) \tag{20}$$

$\phi_m(n)$ is the phase factor applied to subcarrier n in the copy m. For each PTS copy $x_m(t)$, the PAPR is given by:

$$PAPR_m = \frac{\max\left(|x_m(t)|^2\right)}{E\left(|x_m(t)|^2\right)} \tag{21}$$

Let us utilize BFA to represent each bacterium with a set of M phase factor vectors $\{\phi_1, \ldots, \phi_M\}$. The objective function minimizes the average PAPR across all copies.

$$f(\phi) = \frac{1}{M} \cdot \sum_{m} PAPR_m \tag{22}$$

Chemotaxis is utilized to calculate fitness based on objective function is given by:

$$\theta(i, j, k, l) = \exp\left(-\theta_c \cdot J(i, j, k, l)\right), \tag{23}$$

where $\theta(i, j, k, l)$ is the probability of bacterial i tumbling towards the food source in step j of chemotaxis loop k at iteration l, θ_c is the chemotaxis step size, and $J(i, j, k, l)$ is the attractant value for bacterium i at the current step and iteration. The hybrid OTFS signal X_{hybrid} is implemented by merging the optimized and unprocessed segments. The hybrid PTS and BFA approach to reduce the OTFS PAPR can be represented as:

$$x_{\text{hybrid}} = \bigcup_{m=1}^{M} \left(\acute{x}_m \bigcup x_m\right) \tag{24}$$

where x_{hybrid} is the hybrid OTFS signal, $\acute{x}_m$ represents the optimized segments obtained from the PTS using the BFA, and x_m denotes the original input signal not subjected to the PTS.

E. PROPOSED SLM-BFA

Hybridization of SLM with BFA presents significant advantages in terms of PAPR reduction for waveforms. The SLM selectively mitigates the PAPR by generating multiple versions of the transmitted signal and selecting the version with the lowest PAPR. However, determining the optimal phase sequences for PAPR reduction can be computationally intensive, and may not guarantee global optimality. Integrating the BFA enhances the SLM technique by efficiently exploring a more extensive solution space. The adaptive search strategy and robustness of BFA in handling dynamic environments enable it to find better phase sequences for PAPR reduction while reducing computational complexity.

The hybrid approach can also provide a more robust and reliable PAPR reduction in scenarios where conventional SLM techniques may struggle. Overall, hybrid SLM with BFA offers improved PAPR reduction performance, reduced computational complexity, and enhanced adaptability, making it a promising solution for 5G frameworks. The drawbacks of the hybrid SLM with BFA include increased computational complexity owing to the combination of the two optimization techniques. Additionally, tuning the parameters of both SLM and BFA for optimal performance can be challenging, requiring careful consideration and extensive computational resources—the proposed SLM-BFA is given in Fig. 3.

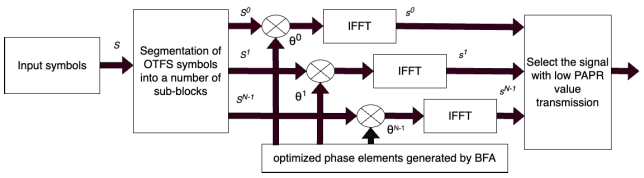

FIGURE 3. SLM-BFA.

Let $x(t)$ be the input signal to the OTFS system and $y(t)$ be the output signal after applying SLM-BFA for PAPR reduction. The PAPR of a signal $x(t)$ can be represented as

$$PAPR(x(t)) = \frac{\max |x(t)|^2}{\mathrm{E}\left\{|x(t)|^2\right\}} \tag{25}$$

The main objective of SLM-BFA is to minimize the PAPR of the signal by optimizing the phase factors. This can be formulated as an optimization problem.

$$\min_{\theta} PAPR\left(x(t)e^{j\theta}\right) \tag{26}$$

where θ is the phase factor applied to the signal. To incorporate the BFA for optimization, let x_i represent the i-th bacteria and $x_i(t)$ represent the signal corresponding to the i-th bacteria. The position of each bacterium x_i can be expressed as a vector of phase factors θ_i. The following equations represent the movement of the bacteria

$$x_i(t + 1) = x_i(t) + \beta \cdot \Delta x_i(t) \tag{27}$$

where β is the step size, and $x_i(t)$ represents the change in the position of the bacteria, which is determined by the chemoattractant and chemorepellent. The swarming is given by

$$x_i(t + 1) = x_i(t) + \alpha \cdot \sum_{j=1}^{N} \left(x_j(t) - x_i(t)\right) \tag{28}$$

The reproduction of the bacterium is given by

$$x_i(t + 1) = \begin{cases} x_{i,t} + \delta & \text{if } P_i > P_{t,x_{i,t}} \\ x_{i,t} - \delta & \text{otherwise} \end{cases} \tag{29}$$

P_i represents the fitness of the i-th bacteria, P_t represents a predetermined threshold, and δ represents the step size for reproduction. Fitness function P_i can be defined as the inverse of the PAPR of the signal corresponding to the i-th bacteria. After several iterations of the BFA, the optimal phase factors

(θ^*) that minimizes the PAPR of the signal can be obtained, and the output signal y(t) can be generated as:

$$y(t) = x(t)e^{j\theta^*} \tag{30}$$

This mathematical model represents the application of SLM-BFA for PAPR reduction in OTFS modulation. The BFA optimizes the phase factors to minimize the PAPR of the signal, thereby improving the efficiency of the OTFS communication system.

Conventional techniques, such as SLM, PTS, clipping, and companding methods, such as the A-law and μ-law, provide fundamental solutions for signal processing tasks, which offer adaptive optimization capabilities, potentially enhancing the performance and efficiency of modulation and PAPR reduction techniques under varying channel conditions. However, the choice between these methods depends on specific application requirements, including trade-offs between complexity, performance, and implementation. Table 1 compares the proposed algorithms with existing methods [34], [35].

III. SIMULATION RESULTS

The proposed hybrid methods, SLM-BFA and PTS-BFA for OTFS, were implemented and analyzed by using Matlab-2016. The simulation analysis consists of 20000 samples, 256-FFT, 256-QAM, and OTFS waveforms with Rayleigh channels. In Fig. 4, we analyzed the performance of the proposed hybrid and conventional algorithms for OTFS waveforms with Rayleigh channels and 64 subcarriers. The main objective was to determine the optimal PAPR obtained at a 10^{-3} CCDF. It is seen that at the CCDF of 10^{-3}, the PAPR of 3 dB, 3.8 dB, 4.8 dB, 6.4 dB, 8.8 dB, and 9.7 dB were obtained by the PTS-BFA $s = 4$, SLM-BFA $s = 4$, PTS-BFA, SLM-BFA, SLM and PTS as compared with the conventional OTFS (10.9 dB). It can be observed that the proposed algorithms SLM-BFA and PTS-BFA outperformed the conventional methods and obtained superior performance. The reduction in PAPR was further improved by increasing the number of sub-blocks. However, increasing the number of sub-blocks may result in a high complexity. Hence, in this study, the sub-blocks were limited to 4. In conclusion, the proposed algorithm achieved a PAPR reduction of 6.1 dB when compared to OTFS modulation in the absence of specific PAPR reduction techniques.

PAPR analysis in Rician channels is crucial for efficient power amplifier design in mobile communications. It helps to predict rare, high-power signal peaks caused by the channel, thereby preventing costly clipping and distortion. In Fig. 5, we have analyzed the PAPR of OTFS with the Rician Channel for 64 subcarriers. In this case, the PAPR of 1.98 dB by PTS-BFA $s = 4$, 2.5 dB PTS-BFA-$s = 4$, 3.7 dB PTS-BFA, 4.7 dB SLM-BFA, 6.3 dB SLM, 8.1 dB PTS, and 10.4 dB (OTFS) were obtained at the CCDF of 10^{-3}. The proposed hybrid algorithm provides superior performance compared to conventional methods. The Hybrid PTS-BFA $s - 4$ obtained a significant PAPR gain of 6.1, 4.5, and 8.6 dB compared to the conventional PTS, SLM, and OTFS. The PTS-BFA $s = 4$ in the Rician Channel obtained a gain of 1.2 dB as compared with the PTS-BFA $s - 4$ in the Rayleigh channel.

TABLE 1. Comparison of proposed algorithms with existing methods.

PAPR Algorithms	Remarks
SLM	1) Utilizes amplitude modulation techniques for signal transmission. 2) Typically involves the modulation of a carrier signal with the information signal to achieve desired signal characteristics. 3) Effective in simple modulation scenarios but may suffer from inefficiency in more complex signal environments.
PTS	1) Partial Transmit Sequence is a technique used in multi-carrier signal processing to reduce PAPR in OFDM systems. 2) It divides the data into several sub-blocks, and phase sequences are applied to each sub-block to minimize the overall PAPR. 3) Provides significant reduction in PAPR at the cost of increased computational complexity.
Clipping and Filtering	1) Involves clipping the peaks of a signal to reduce its dynamic range, followed by filtering to remove distortion introduced by clipping. 2) Provides a simple and effective means of reducing signal peaks, but may introduce signal distortion and degrade signal quality, especially for high clipping levels.
A-law and μ-law	1) Companding techniques used in telecommunication systems to compress dynamic range. 2) A-law and μ-law are nonlinear quantization algorithms that allocate more bits to lower-amplitude signals and fewer bits to higher-amplitude signals. 3) Widely used in digital telephony systems, particularly in PCM (Pulse Code Modulation) encoding, to achieve a more uniform signal-to-noise ratio across a wide range of signal amplitudes.
Proposed SLM-BFA	1) Inspired by the foraging behavior of bacteria, SLM-BFA optimizes the performance of SLM systems by dynamically adjusting modulation parameters based on environmental conditions. 2) Provides adaptive modulation, allowing for efficient utilization of the available channel resources and improved system performance under varying channel conditions. 3) Offers potential improvements in spectral efficiency and error performance compared to conventional SLM techniques.
Proposed PTS-BFA	1) Similar to SLM-BFA, PTS-BFA optimizes the performance of PTS systems by dynamically adjusting phase sequences based on environmental conditions. 2) Provides adaptive PAPR reduction, allowing for efficient reduction of peak power while maintaining signal quality. 3) Offers potential improvements in PAPR reduction efficiency and computational complexity compared to conventional PTS techniques.

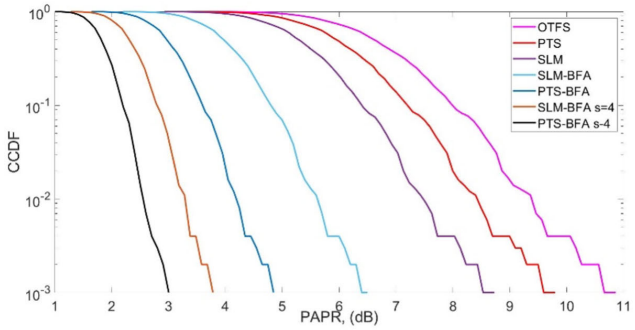

FIGURE 4. PAPR in rayleigh channel with 64 subcarriers.

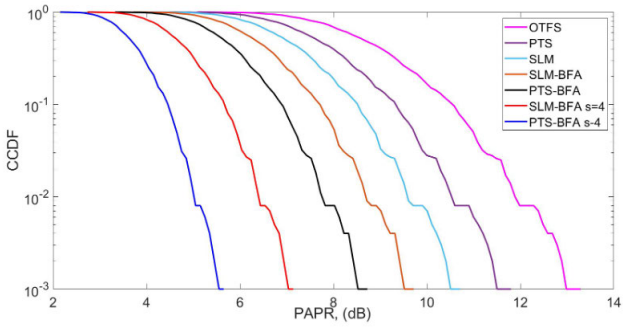

FIGURE 6. PAPR in rayleigh channel with 256-subcarriers.

TABLE 2. PAPR comparison of rayleigh and rician channel for 64-subcarriers.

Algorithms	PAPR (dB) at 10^{-3} (Rayleigh Channel)	PAPR (dB) at 10^{-3} (Rician Channel)	PAPR gain (dB) in Rician Channel
OTFS	10.9	10.6	0.3
PTS	9.7	8.1	1.6
SLM	8.8	7.3	1.5
SLM-BFA	6.4	4.4	2
PTS-BFA	4.8	3.9	0.9
SLM-BFA S=4	3.8	2.6	1.2
PTS-BFA S=4	3	1.8	1.2

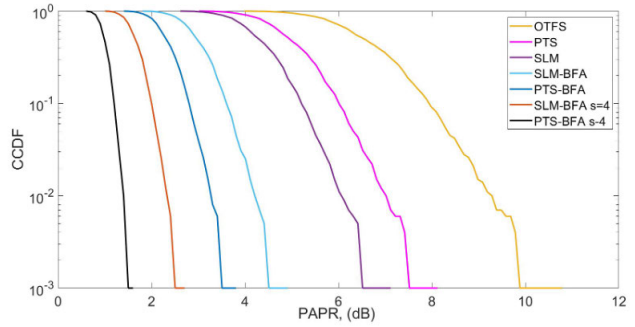

FIGURE 5. PAPR in rician channel with 64 subcarriers.

Therefore, it is deduced that the proposed hybrid schemes exhibit enhanced performance in Rician fading environments compared to Rayleigh fading environments. Table 2 presents the numerical analysis results shown in Fig. 4 and 5.

Utilization of a large number of subcarriers boosts the spectral efficiency (data per Hz) by 33%. This translates to higher data rates without requiring more spectrum, which is crucial for supporting diverse 5G applications but also increases the PAPR of the framework. Hence, it is essential to estimate the performance of the proposed methods for an OTFS waveform with a Rayleigh channel and 256 subcarriers, as shown in Fig. 6. At the CCDF of 10^{-3}, the PAPR obtained by OTFS (13.2 dB) is reduced to 5.7 dB by PTS-BFA $s = 4$, 7.1 dB by SLM=BFA $s = 4$, 8.4 dB by PTS-BFA, 9.2 dB by SLM-BFA, 10.3 dB by SLM, and 11.7 dB by PTS. The proposed PTS-BFA $s = 4$ outperforms the OTFS by obtaining a PAPR gain of 7.5 dB. It is also noted that the PAPR performance of the 64 subcarriers is better than that of the 256 subcarriers. Hence, it is concluded that 64 subcarriers generally offer a lower PAPR; the specific context, including modulation, coding, and desired data rate, determines the optimal choice. Two hundred fifty-six subcarriers may be necessary to achieve higher data rates, requiring advanced PAPR management techniques.

In Fig. 7, the PAPR of an OTFS waveform with a Rician Channel and 256 subcarriers are analyzed for different PAPR minimization techniques. The primary objective of this analysis was to quantify the reduction in the PAPR by the Rician Channel relative to the Rayleigh Channel. The PAPR of the OTFS without using PAPR reduction algorithms is 13.7 dB at the CCDF of 10^{-3}, which is minimized to 5.1 dB by PTS-BFA $s = 4$, 6.3 dB by SLM-BFA $s = 4$, 8.1 dB by PTS-BFA, 9.7 dB by SLM-BFA, 10.3 dB by SLM, and 11.8 dB by PTS. Hence, it is concluded that the proposed hybrid algorithms achieves an optimal PAPR performance. The Rayleigh channel represents a typical scattered mobile environment, leading to random signal fluctuations and a higher potential for extreme peaks in 256 subcarriers owing to more constructive interference possibilities. PAPR analysis here critical for the amplifier design and potential PAPR reduction techniques. Conversely, the Rician Channel incorporates a pronounced line-of-sight (LOS) component in addition to the scattered signals, rendering the channel less random and typically leading to a lower PAPR in comparison to Rayleigh fading. While still necessary, PAPR analysis might be less critical, depending on LOS strength. Table 3 presents the numerical analysis results shown in Fig. 6 and 7.

The reduction in PAPR in the 5G's OTFS waveforms increases the BER. This is a trade-off between amplifier efficiency and potential signal degradation. The PAPR method lowers the peaks for amplifier safety, but also introduces slight signal modifications that could increase the BER value, which degrades the performance of the framework. Hence, it is essential to analyze the throughput performance of the framework for the proposed algorithms under different channel conditions. The main objective is to maintain the BER performance of the OTFS while lowering the PAPR. A BER analysis of the Rayleigh channels for the

TABLE 3. PAPR comparison of rayleigh and rician channel for 256-subcarriers.

Algorithm	PAPR (dB) at 10^{-3} (Rayleigh Channel)	PAPR (dB) at 10^{-3} (Rician Channel)	PAPR gain (dB) in Rician Channel
OTFS	13.2	13.7	0.5
PTS	11.8	11.7	0.1
SLM	10.5	10.3	0.2
SLM-BFA	9.2	9.7	0.5
PTS-BFA	8.6	8.1	0.5
SLM-BFA S=4	7.1	6.3	0.8
PTS-BFA S=4	5.7	4.8	0.9

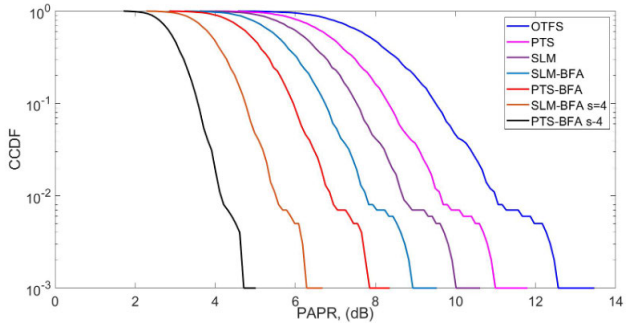

FIGURE 7. PAPR in rician channel with 256-subcarriers.

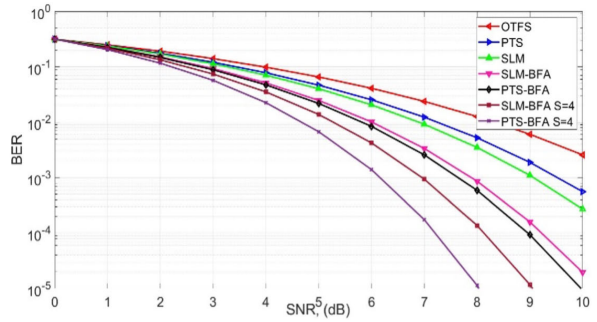

FIGURE 8. BER 64 subcarriers rayleigh channel.

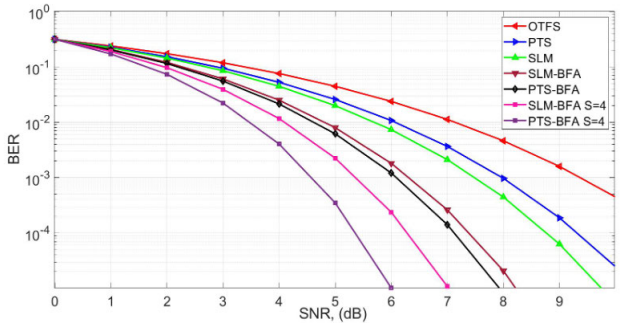

FIGURE 9. BER 64 subcarriers rician channel.

TABLE 4. BER comparison of rayleigh and rician channel for 64-subcarriers.

Algorithms	SNR (dB) at BER of 10^{-3} (Rayleigh Channel)	SNR (dB) at BER of 10^{-3} (Rician Channel)	SNR gain (dB) in Rician Channel
OTFS	10.8	9.5	0.3
PTS	9.7	8	1.7
SLM	9.1	7.5	1.4
SLM-BFA	7.9	6.4	1.5
PTS-BFA	7.6	6.1	1.5
SLM-BFA S=4	7	5.4	1.6
PTS-BFA S=4	6.2	4.8	1.4

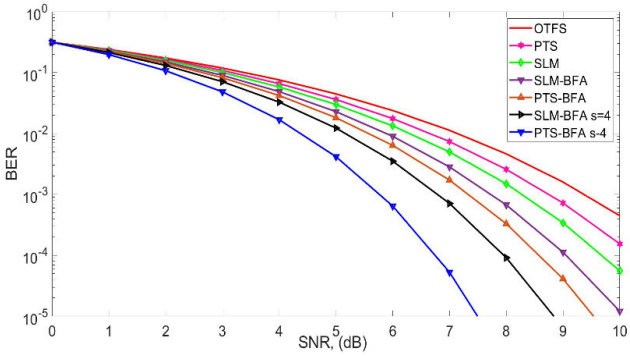

FIGURE 10. BER 256 subcarriers rayleigh channel.

64 subcarriers is shown in Fig. 8. It is seen that the PAPR of 10.8 dB, 9.7 dB, 9.1 dB, 7.9 dB, 7.6 dB, 7 dB, and 6.2 dB are obtained by the conventional and proposed algorithms at the CCDF of 10^{-3}. The PTS-BFA and SLM-BFA obtained a PAPR gain of 4.6 dB and 3.8 dB as compared to the OTFS signal (10.8 dB). Hence, it can be concluded that the proposed schemes efficiently retain the BER of the framework.

In Fig. 9, we analyzed the BER of an OTFS waveform for 64 subcarriers with a Rician channel for different PAPR schemes. The CCDF of 10^{-3} is obtained at the PAPR of 9.5 dB by OTFS which is further reduced to 4.8 dB by PTS-BFA, 5.4 dB by PTS-BFA, 6.1 dB by SLM-BFA, 6.4 dB by PTS-BFA, 7.5 dB by PTS, and 8 dB by SLM respectively. The performance of the PAPR schemes in the Rician channel is better than that in the Rayleigh channel. Hence, it can be concluded that the proposed hybrid method efficiently improved the performance of the framework. Table 4 presents the numerical analysis results shown in Fig. 8 and 9.

In Fig. 10, we estimate the BER curves of an OTFS waveform with a Rayleigh channel for 256 subcarriers. The BER of 10^{-5} is obtained at the SNR of 7.4 dB by PTS-BFA $s = 4$, 8.8 dB by SLM-BFA $s = 4$, 9.6 dB by PTS-BFA, 10.2 dB by SLM-BFA, 13 dB by SLM, 14.1 dB by PTS, and 15.2 dB for the OTFS waveform. It was confirmed that the proposed PTS-BFA $s = 4$ obtained an SNR gain of 8.2 dB at 10^{-5} (CCDF). Therefore, the results demonstrate that the proposed algorithms maintain BER performance while reducing the PAPR of the system.

Fig. 11 illustrates the analysis of the BER performance for an OTFS waveform under the influence of a Rician Channel utilizing 256 subcarriers. SNR of 7.2 dB, 8.1 dB, 8.8 dB,

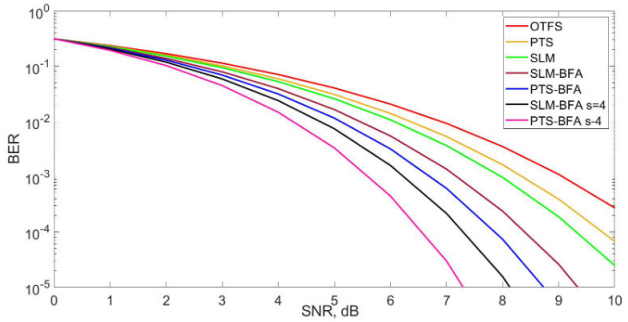

FIGURE 11. BER with 256 subcarriers rician channel.

TABLE 5. BER comparison of rayleigh and rician channel for 256-subcarriers.

Algorithms	SNR (dB) at BER of 10^{-3} (Rayleigh Channel)	SNR (dB) at BER of 10^{-3} (Rician Channel)	SNR gain (dB) in Rician Channel
OTFS	15.2	12.3	3.1
PTS	14.1	11.1	3.0
SLM	13.0	10.9	2.1
SLM-BFA	10.2	9.3	0.9
PTS-BFA	9.6	8.8	0.8
SLM-BFA S=4	8.8	8.1	0.7
PTS-BFA S=4	7.4	7.2	0.2

TABLE 6. PSD comparison of rayleigh and rician channel for 256-subcarriers.

Algorithms	SNR (dB) at BER of 10^{-3} (Rayleigh Channel)	SNR (dB) at BER of 10^{-3} (Rician Channel)	PSD gain (dB) in Rician Channel
OTFS	-480	-600	-120
PTS	-610	-780	-170
SLM	-780	-860	-80
SLM-BFA	-830	-900	-70
PTS-BFA	-970	-1050	-80
SLM-BFA S=4	-1075	-1100	-25
PTS-BFA S=4	-1190	-1380	-190

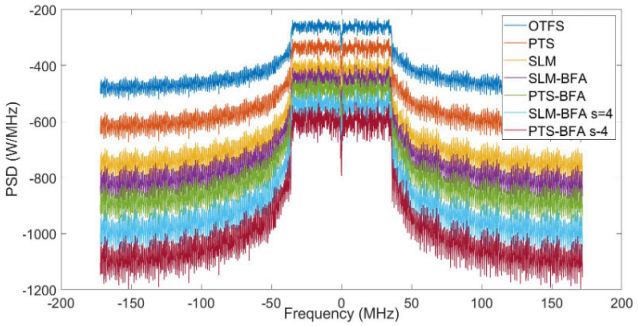

FIGURE 12. PSD with 256 subcarriers rayleigh channel.

9.3 dB, 10.9 dB, 11.1 dB, and 12.2 dB are obtained by the dB by PTS-BFA $s = 4$, SLM=BFA $s = 4$, PTS-BFA, SLM-BFA, SLM, PTS and OTFS. Hence, it is concluded that the proposed PTS-BFA $s = 4$ outperforms the conventional and contemporary algorithms. Therefore, the proposed method successfully retained the BER performance. Rician channels generally offer a better BER performance than Rayleigh channels because a vital, direct LOS component in the Rician channels stabilizes the received signal. This reduces the deep fades experienced in Rayleigh channels, where scattered signals constantly fluctuate, weakening the signal and increasing errors. The LOS component effectively boosts the SNR compared to Rayleigh channels, providing a more substantial margin for errors to be overcome. This directly translates to an improved BER performance, meaning that fewer bits are flipped during the transmission. However, the benefits of an LOS component depend on its strength. The Rician Channel can approach Rayleigh-like behavior in weak LOS scenarios, thereby diminishing the BER advantage. Other factors, such as modulation schemes and coding techniques, also influence BER performance. Table 5 presents the numerical analysis results shown in Fig. 10 and 11.

OTFS waveforms aim to spread signal energy across time and frequency, thereby improving resilience in Rayleigh channels (prone to signal fluctuations). The proposed hybrid algorithms can enhance this resilience further. However, their impact on the power spectrum density, which is related to the signal distribution across frequencies, depends on the channel conditions. The PSD of the OTFS waveform with the Rayleigh channel and 256 subcarriers were estimated and analyzed, as shown in Fig. 12. The PSD values of -480, -610, -780, -830, -970, -1075, and -1190 were obtained using the OTFS, PTS, SLM, SLM-BFA, PTS-BFA, SLM-BFA $s = 4$ and PTS-BFA $s = 4$ methods. Hence, it should be noted that the proposed PTS-BFA $s = 4$ obtained a gain of -720 compared with OTFS (without PAPR methods).

PSD refers to the distribution of signal power across frequencies. In 5G, improving the PSD can boost the throughput by packing more data, which allows more information to be crammed into the same frequency band. Improving the PSD minimizes the overlap with neighboring signals, prevents data corruption, and ensures smoother communication. The generated power distribution enables sharper beams to focus on specific users, maximize data delivery, and minimize spectrum leakage. PSD optimization in 5G unlocks significant throughput improvements, paving the way for faster and more reliable data transfers. The PSD of the OTFS waveform with a Rayleigh channel and 256 subcarriers is shown in Fig. 13. The PSD values of -600, -780, -860, -900, -1050, -1100, and -1380, obtained by the OTFS, PTS, SLM, SLM-BFA, PTS-BFA, SLM-BFA $s = 4$, and PTS-BFA $s = 4$ methods, respectively, showed that the spectrum leakage was efficiently minimized as compared with the OTFS. The lowering of spectrum leakage allows more subcarriers to accommodate, which, in turn, enhances the framework's spectral access to the framework. Table 6 presents the numerical analysis results in Fig. 12 and 13.

TABLE 7. Comparison of proposed methods with existing PAPR conventional methods.

Ref.	PAPR Algorithms	SNR at the BER of 10^{-3}	PAPR at CCDF of 10^{-3}	PSD estimation	Channel
[36]	Self-Adjustment gain method in OFDM	10 dB and 10.5	8.5 dB and 9.8 dB	No	Rayleigh
[37]	H-SLM for OFDM	8.8 dB	9.5 dB	No	Rayleigh
[14]	SLM for OFDM-NOMA	22 dB	7.1 dB	No	Rayleigh
[39]	Clipping for OFDM-NOMA	NA	11 dB	No	Rayleigh
[40]	Zadof Chu Transform for NOMA	11 dB	6.4 dB	No	Rayleigh
[41]	Companding method in FBMC	12.3	7.6 dB	No	Rayleigh
[42]	Clipping Method for FBMC	20 dB	6.6 dB	No	Rayleigh
[7]	OTFS	Not simulated	9.8	No	Rayleigh
[44]	OTFS with SLM (S=2)	Not simulated	10.12	No	Rayleigh
[45]	OTFS signal using airy special function	Not simulated	9.2 dB	No	Rayleigh
[3]	OTFS PAPR preamble	21 dB	11	No	Rayleigh
[16]	PTS-PSO for OFDM	No simulated	5.8	No	Rayleigh
Proposed Method	OTFS with SLM-BFA for 64 subcarriers with Rician and Rayleigh channel	5.4 and 7	2.6 and 3.8 dB	No	Rician and Rayleigh channel
Proposed Method	OTFS with PTS-BFA for 64 subcarriers with Rician and Rayleigh channel	4.8 and 6.2	1.8 and 3	No	Rician and Rayleigh channel
Proposed Methods	OTFS with SLM-BFA for 256 subcarriers	8.1 and 8.8	6.3 and 7.1 dB	-1075 and -1100	Rician and Rayleigh channel
Proposed Methods (PTS-BFA)	OTFS with PTS-BFA for 256 subcarriers	7.2 and 7.4	4.8 and 5.7	-1190 and -1380	Rician and Rayleigh channel

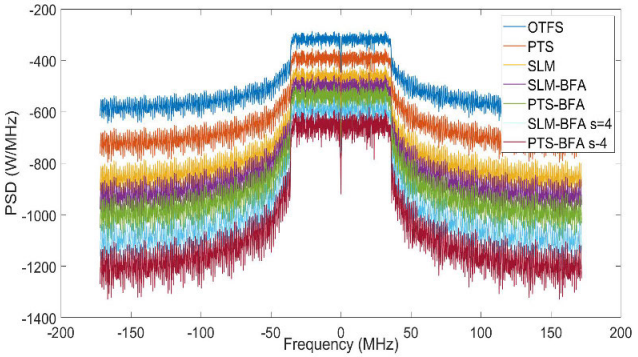

FIGURE 13. PSD with 256 subcarriers rician channel.

TABLE 8. Complexity analysis.

No.	PAPR algorithms	Complexity
1	PTS	$O(N * M)$ complexity, where N is the number of subcarriers and M is the number of candidate phase shifts.
2	SLM	$O(N^2 * S)$ complexity, where N is the number of subcarriers and S is the number of symbols.
3	PTS-BFO	$O((N * M) +$ (population_size $*$ generation)) where for BFO optimization, where population_size is the number of bacteria and generation is the number of iterations.
4	SLM-BFO	$O((N^2 * S) +$ (population_size $*$ generation))

The conventional PAPR algorithms utilized in OFDM cannot be used in the other advanced waveforms owing to their differences in the structural arrangement. Therefore, a unique PAPR algorithm must be implemented based on a particular waveform design. Furthermore, in the OTFS waveform, to the best of our knowledge and available literature, PAPR reduction using hybrid algorithms such as PTS-BFA and SLM-BFA has been used for the first time in the proposed work. Recent studies on PAPR have analyzed the BER and PAPE performance in the Rayleigh channel; however, in this work, we have analyzed PAPR, BER, and PSD with 64 and 256 subcarriers for both the Rician and Rayleigh channels. In recent publications, it has been observed that the BER performance is degraded while lowering the complexity and PAPR; however, in this work, we have seen that the BER performance is retained for 64 and 256 subcarriers without compromising the PAPR performance. Table 7 presents a comparison between the proposed and published methods.

A. COMPLEXITY

PAPR reduction algorithms battle high-peak power transmissions to achieve efficiency. However, this fight comes at a cost complexity. The PTS and SLM are popular techniques that trade effectiveness in terms of complexity. PTS checks many phase combinations (NM), whereas SLM compares symbol mappings (N^2S), both of which are costly for large systems. Enter optimization algorithms, such as BFA. They search for optimal solutions, such as PTS and SLM, but with a twist, they learn and evolve. This can reduce the number of evaluations required, thus reducing the complexity (population_size $*$ generation). However, the complexity cost is shifted to maintaining the "bacteria" population.

Complexity is important because real-time systems require high speeds. Choosing the right algorithm depends on balance: brute-force effectiveness (PTS, SLM) or strategic search with trade-offs (PTS-BFO, SLM-BFO). Table 8 presents the complexity analysis of the conventional and PAPR algorithms.

IV. CONCLUSION

This article presents the PTS-BFA and SLM-BFA algorithms to lower the PAPR value while retaining the BER and PSD performance of an OTFS waveform for Rayleigh and Rician channels. Both hybrid algorithms have the potential to contribute significantly to the PAPR reduction in OTFS systems. Observations reveal that the BFA explicitly explores the optimal phase factors for individual subcarriers within the PTS scheme, resulting in a reduced PAPR when compared with the random or fixed phase values typically employed in conventional PTS techniques. By intelligently exploring the search space, BFO avoids reqruiring a computationally expanded exhaustive search for optimal phase factors. The SLM-BFA can optimize the allocation of data symbols to the classifiers in the SLM scheme, thereby minimizing the potential for high-power peaks. By dynamically adjusting the symbol allocation based on the PAPR characteristics, SLM-BFA can outperform static allocation methods. Both PTS-BFO and SLM-BFO show promise for a significant PAPR reduction in OTFS. Their strengths and potential for synergistic combination make them valuable tools for researchers and engineers to explore improved PAPR performance in OTFS-based communication systems. Additionally, augmenting the number of subcarriers can yield optimal PAPR, albeit at the expense of heightened complexity within the framework. However, the effectiveness of these algorithms can be influenced by factors such as the number of subcarriers, the modulation scheme, and the channel characteristics. Further research is required to explore the optimal integration of BFO with other PAPR reduction techniques in OTFS systems.

REFERENCES

[1] A. Gunturu, A. R. Godala, A. K. Sahoo, and A. K. R. Chavva, "Performance analysis of OTFS waveform for 5G NR mmWave communication system," in *Proc. IEEE Wireless Commun. Netw. Conf. (WCNC)*, Mar. 2021, pp. 1–6.

[2] H. B. Mishra, P. Singh, A. K. Prasad, and R. Budhiraja, "OTFS channel estimation and data detection designs with superimposed pilots," *IEEE Trans. Wireless Commun.*, vol. 21, no. 4, pp. 2258–2274, Apr. 2022.

[3] V. Baena-Lecuyer, A. C. O. Oria, and J. G. Romero, "Low PAPR preamble-based channel estimation for OTFS systems on static multipath channels," *Digit. Signal Process.*, vol. 136, May 2023, Art. no. 103979.

[4] M. Attaran, "The impact of 5G on the evolution of intelligent automation and industry digitization," *J. Ambient Intell. Humanized Comput.*, vol. 14, no. 5, pp. 5977–5993, May 2023.

[5] T. Sun, J. Lv, and T. Zhou, "A transformer-based channel estimation method for OTFS systems," *Entropy*, vol. 25, no. 10, p. 1423, Oct. 2023.

[6] M. Li, W. Liu, and J. Lei, "A review on orthogonal time–frequency space modulation: State-of-art, hotspots and challenges," *Comput. Netw.*, vol. 224, Apr. 2023, Art. no. 109597.

[7] G. D. Surabhi, R. M. Augustine, and A. Chockalingam, "Peak-to-average power ratio of OTFS modulation," *IEEE Commun. Lett.*, vol. 23, no. 6, pp. 999–1002, Jun. 2019.

[8] A. Abushattal, S. E. Zegrar, A. Yazgan, and H. Arslan, "A comprehensive experimental emulation for OTFS waveform RF-impairments," *Sensors*, vol. 23, no. 1, p. 38, 2022.

[9] H. Bitra, P. Ponnusamy, S. Chintagunta, and S. Pragadeshwaran, "Nonlinear companding transforms for reducing the PAPR of OTFS signal," *Phys. Commun.*, vol. 53, Aug. 2022, Art. no. 101729.

[10] E. D. P. Chechi, "Performance comparison of BPSO and BFO algorithms of PTS technique used for PAPR reduction in MC-CDMA," *Int. J. Eng. Res.*, vol. 4, no. 6, pp. 300–302, Jun. 2015.

[11] A. Kumar, "Analysis of PAPR on NOMA waveforms using hybrid algorithm," *Wireless Pers. Commun.*, vol. 132, no. 3, pp. 1849–1861, Oct. 2023.

[12] A. Kumar, K. Rajagopal, N. Alruwais, H. M. Alshahrani, H. Mahgoub, and K. M. Othman, "PAPR reduction using SLM-PTS-CT hybrid PAPR method for optical NOMA waveform," *Heliyon*, vol. 9, no. 10, Oct. 2023, Art. no. e20901.

[13] R. Sayyari, J. Pourrostam, and H. Ahmadi, "Efficient PAPR reduction scheme for OFDM-NOMA systems based on DSI & precoding methods," *Phys. Commun.*, vol. 47, Aug. 2021, Art. no. 101372.

[14] M. Mounir, M. I. Youssef, and A. M. Aboshosha, "Low-complexity selective mapping technique for PAPR reduction in downlink power domain OFDM-NOMA," *EURASIP J. Adv. Signal Process.*, vol. 2023, no. 1, p. 10, Jan. 2023.

[15] K. Chandekar and V. Nithya, "Hybrid PAPR reduction using Hartley transform pre-coding with clipping and filtering technique in OFDM-NOMA system," *Int. J. Electr. Eng. Technol.*, vol. 11, no. 4, pp. 341–348, Apr. 2020.

[16] M. H. Aghdam and A. A. Sharifi, "PAPR reduction in OFDM systems: An efficient PTS approach based on particle swarm optimization," *ICT Exp.*, vol. 5, no. 3, pp. 178–181, Sep. 2019.

[17] M. Liu, W. Chen, J. Xu, and B. Ai, "A comprehensive study of PAPR reduction techniques for deep joint source channel coding in OFDM systems," in *Proc. IEEE 23rd Int. Conf. Commun. Technol. (ICCT)*, Oct. 2023, pp. 1395–1399.

[18] F. Zou, Z. Liu, X. Hu, and G. Wang, "A novel PAPR reduction scheme for OFDM systems based on neural networks," *Wireless Commun. Mobile Comput.*, vol. 2021, pp. 1–8, Apr. 2021.

[19] V. S. Nagaraju, R. Anusha, and R. R. Vallabhuni, "A hybrid PAPR reduction technique in OFDM systems," in *Proc. IEEE Int. Women Eng. (WIE) Conf. Electr. Comput. Eng. (WIECON-ECE)*, Dec. 2020, pp. 364–367.

[20] N. Gupta and G. Saini, "Performance analysis of BFO for PAPR reduction in OFDM," *Int. J. Soft Comput. Eng.*, vol. 2, no. 5, pp. 2231–2307, 2012.

[21] S. Prasad and R. Jayabalan, "PAPR reduction in OFDM using scaled particle swarm optimisation based partial transmit sequence technique," *J. Eng.*, vol. 2019, no. 5, pp. 3460–3468, May 2019.

[22] A. Abdalmunam, M. S. Anuar, M. N. Junta, N. M. Nawawi, and A. Noori, "Implementation of particle swarm optimization and genetic algorithms to tackle the PAPR problem of OFDM system," *IOP Conf. Ser., Mater. Sci. Eng.*, vol. 767, Feb. 2020, Art. no. 012030.

[23] A. Kumar, N. Gaur, M. Mallam, and A. Nanthaamornphong, "Enhancing the power amplifier performance of an optical-OTFS modulation for optical communication system," *J. Opt. Commun.*, pp. 1–7, Feb. 2024, doi: 10.1515/joc-2023-0378.

[24] R. Hadani, S. Rakib, A. F. Molisch, C. Ibars, A. Monk, M. Tsatsanis, J. Delfeld, A. Goldsmith, and R. Calderbank, "Orthogonal time frequency space (OTFS) modulation for millimeter-wave communications systems," in *IEEE MTT-S Int. Microw. Symp. Dig.*, Jun. 2017, pp. 681–683.

[25] Y. Rahmatallah and S. Mohan, "Peak-to-average power ratio reduction in OFDM systems: A survey and taxonomy," *IEEE Commun. Surveys Tuts.*, vol. 15, no. 4, pp. 1567–1592, 4th Quart., 2013.

[26] H. K. Sinha, A. Kumar, and D. Pradhan, "A study of various peak to average power ratio (PAPR) reduction techniques for 5G communication system (5G-CS)," in *Optimization Techniques in Engineering: Advances and Applications*. Hoboken, NJ, USA: Wiley, 2023, pp. 437–454.

[27] M. Mounir, M. B. El Mashade, A. M. Aboshosha, and M. I. Youssef, "Impact of HPA nonlinearity on the performance of power domain OFDM-NOMA system," *Eng. Res. Exp.*, vol. 4, no. 2, Jun. 2022, Art. no. 025004.

[28] A. Kumar, "PAPR reduction in beyond 5G waveforms using a novel SLM algorithm," *Nat. Acad. Sci. Lett.*, vol. 46, no. 6, pp. 535–538, Dec. 2023.

[29] P. Gupta and H. P. Thethi, "Performance investigations and PAPR reduction analysis using very efficient and optimized amended SLM algorithm for wireless communication OFDM system," *Wireless Pers. Commun.*, vol. 115, no. 1, pp. 103–128, Nov. 2020.
[30] K. M. Passino, "Biomimicry of bacterial foraging for distributed optimization and control," *IEEE Control Syst. Mag.*, vol. 22, no. 3, pp. 52–67, Jun. 2002.
[31] O. P. Verma, M. Hanmandlu, A. K. Sultania, and A. S. Parihar, "A novel fuzzy system for edge detection in noisy image using bacterial foraging," *Multidimensional Syst. Signal Process.*, vol. 24, pp. 181–198, Mar. 2013.
[32] S. Mishra and C. N. Bhende, "Bacterial foraging technique-based optimized active power filter for load compensation," *IEEE Trans. Power Del.*, vol. 22, no. 1, pp. 457–465, Jan. 2007.
[33] S. Das, A. Biswas, S. Dasgupta, and A. Abraham, "Bacterial foraging optimization algorithm: Theoretical foundations, analysis, and applications," in *Foundations of Computational Intelligence Volume 3: Global Optimization*. Berlin, Germany: Springer, 2009, pp. 23–55.
[34] A. Kumar, S. Chakravarty, and A. Nanthaamornphong, "Analysis of PAPR reduction of optical-OTFS for 256-QAM using companding and clipping–filtering algorithms," *J. Opt. Commun.*, pp. 1–8, Jan. 2024, doi: 10.1515/joc-2023-0369.
[35] X. Ma, W. Raza, Z. Wu, M. Bilal, Z. Zhou, and A. Ali, "A nonlinear distortion removal based on deep neural network for underwater acoustic OFDM communication with the mitigation of peak to average power ratio," *Appl. Sci.*, vol. 10, no. 14, p. 4986, Jul. 2020.
[36] M.-J. Hao and W.-W. Pi, "PAPR reduction in OFDM signals by self-adjustment gain method," *Electronics*, vol. 10, no. 14, p. 1672, Jul. 2021.
[37] N. A. Sivadas, "PAPR reduction of OFDM systems using H-SLM method with a multiplierless IFFT/FFT technique," *ETRI J.*, vol. 44, no. 3, pp. 379–388, Jun. 2022.
[38] T. Tang, Y. Mao, and G. Hu, "A fair power allocation approach to OFDM-based NOMA with consideration of clipping," *Electronics*, vol. 9, no. 10, p. 1743, Oct. 2020.
[39] V. B. Kaba and R. R. Patil, "A precoding based PAPR minimization schemes for NOMA in 5G network," *Social Netw. Comput. Sci.*, vol. 2, no. 4, p. 262, Jul. 2021.
[40] I. A. Shaheen, A. Zekry, F. Newagy, and R. Ibrahim, "Performance evaluation of PAPR reduction in FBMC system using nonlinear companding transform," *ICT Exp.*, vol. 5, no. 1, pp. 41–46, Mar. 2019.
[41] Z. Kollár and P. Horváth, "PAPR reduction of FBMC by clipping and its iterative compensation," *J. Comput. Netw. Commun.*, vol. 2012, pp. 1–11, Mar. 2012.
[42] S. Chennamsetty, S. Boddu, P. Chandhar, and K. C. Bulusu, "Analysis of PAPR in OTFS modulation with classical selected mapping technique," in *Proc. 15th Int. Conf. Commun. Syst. Netw. (COMSNETS)*, Jan. 2023, pp. 319–322.
[43] H. Bitra, C. Anusha, and N. C. Pradhan, "Reduction of PAPR in OTFS signal using airy special function," *J. Opt. Commun.*, pp. 1–13, Sep. 2023.

ARUN KUMAR (Member, IEEE) received the Ph.D. degree in electronics and communication engineering from JECRC University, Jaipur, India. He is currently an Associate Professor of electronics and communication engineering with the New Horizon College of Engineering, Bengaluru, India. He has a total of ten years of teaching experience and has published more than 85 research articles in SCI-E and Scopus index journals. He has successfully implemented different reduction techniques for multi-carrier waveforms, such as NOMA, FBMC, and UFMC, and has also implemented and compared different waveform techniques for the 5G systems. He is working on the requirements of a 5G-based smart hospital systems. His research interests include advanced waveforms for 5G mobile communication systems and 5G-based smart hospitals, PAPR reduction techniques in the multicarrier waveform, and spectrum sensing techniques. He is a reviewer of many refereed and indexed journals.

NISHANT GAUR has been working in the fields of communications engineering, antennas, wireless communications,5G and 6G, electrical and electronics engineering, MATLAB, telecommunications engineering, spectrum sensing, network science, simulink, signal processing, image processing, and material science. Currently, he is an Associate Professor with the Department of Physics, JECRC University, Jaipur, India. He has 23 years of experience in research and as a Professor. His research interests include 5G and 6G, numerical analysis and computer programming, classical mechanics, mechanics, binary alloys, quantum mechanics, and cryptography.

AZIZ NANTHAAMORNPHONG (Member, IEEE) received the Ph.D. degree from The University of Alabama, USA. He is currently an Associate Professor and the Dean of the College of Computing, Prince of Songkla University, Phuket Campus, Thailand. With an extensive academic background, he specializes in machine learning, data science, and among other areas. His research significantly contributes to the development of scientific software and leverages data science in the field of tourism. In addition to his core focus, he is also deeply engaged in the study of communication networks, pioneering innovative approaches to foster a beneficial interplay between humans, and technology.